Physica Medica 30 (2014) 437–447

Contents lists available at ScienceDirect

Physica Medica

journal homepage: http://www.physicamedica.com

Original paper

Towards radiological diagnosis of abdominal adhesions based on motion signatures derived from sequences of cine-MRI images

John Fenner [a,*], Benjamin Wright [a], Jonathan Emberey [a], Paul Spencer [b], Richard Gillott [b], Angela Summers [c], Charles Hutchinson [d], Pat Lawford [a], Paul Brenchley [c], Karna Dev Bardhan [b]

[a] Medical Physics Group, Dept of Cardiovascular Science, University of Sheffield, Beech Hill Road, Sheffield, Sth Yorks. S10 2RX, UK
[b] The Rotherham NHS Foundation Trust, Rotherham Hospital, Moorgate Road, Rotherham S60 2UD, UK
[c] Renal Research Labs, University Dept of Medicine, Manchester Royal Infirmary, Manchester M13 9WL, UK
[d] University of Warwick, Health Sciences, Clifford Bridge Road, Coventry CV2 2DX, UK

ARTICLE INFO

Article history:
Received 10 July 2013
Received in revised form
4 December 2013
Accepted 6 December 2013
Available online 16 January 2014

Keywords:
Abdominal adhesions
Magnetic resonance imaging (MRI)
Image registration
Computer-aided detection and diagnosis
ROC analysis

ABSTRACT

This paper reports novel development and preliminary application of an image registration technique for diagnosis of abdominal adhesions imaged with cine-MRI (cMRI). Adhesions can severely compromise the movement and physiological function of the abdominal contents, and their presence is difficult to detect. The image registration approach presented here is designed to expose anomalies in movement of the abdominal organs, providing a movement signature that is indicative of underlying structural abnormalities. Validation of the technique was performed using structurally based *in vitro* and *in silico* models, supported with Receiver Operating Characteristic (ROC) methods. For the more challenging cases presented to the small cohort of 4 observers, the AUC (area under curve) improved from a mean value of 0.67 ± 0.02 (without image registration assistance) to a value of 0.87 ± 0.02 when image registration support was included. Also, in these cases, a reduction in time to diagnosis was observed, decreasing by between 20% and 50%. These results provided sufficient confidence to apply the image registration diagnostic protocol to sample magnetic resonance imaging data from healthy volunteers as well as a patient suffering from encapsulating peritoneal sclerosis (an extreme form of adhesions) where immobilization of the gut by cocooning of the small bowel is observed. The results as a whole support the hypothesis that movement analysis using image registration offers a possible method for detecting underlying structural anomalies and encourages further investigation.

Introduction

The challenge of diagnosing particular abdominal abnormalities from moving images, supported by analysis using image registration, is the focus of this article. Our interest is the abdominal cavity, which through injury can manifest adhesions. Adhesions can be likened to "internal scars". Sometimes congenital, the majority follow infection, injury (after abdominal operations) or intestinal disease (e.g. Crohn's). The adhesions can resemble a rope, multiple strands of varying thickness or a mesh, tethering together abdominal organs, or an organ to the abdominal wall. They may present in a broad spectrum of forms, from minor irritation to the lethal cocooning of the abdominal contents characteristic of Encapsulating Peritoneal Sclerosis (EPS) [1–4]. It is only when adhesions obstruct the intestine and require surgery that the diagnosis becomes clear; in all other instances adhesions as a cause of recurrent or continuing abdominal pain remains a possibility.

Non-invasive methods of detecting abdominal adhesions are strongly preferred, which is the rationale for the deployment of minimally invasive imaging methods for diagnosis, but this is acknowledged to be very challenging. In the domain of diagnostic imaging, plane film radiography and fluoroscopy are increasingly being replaced by more powerful techniques [5,6] – the use of CT is widely cited [7–11]. However, reliable methods for diagnosis remain illusive. The roles of Ultrasound and Magnetic Resonance Imaging are acknowledged in certain circumstances [6,12–15] and their non-invasive/non-ionising characteristics make them appealing. Recommended practice is to study the movement of the abdominal contents (sometimes enhanced with the use of a contrast medium) and infer the presence of adhesions from the disruptions that might be introduced to the patterns of movement

* Corresponding author. Tel.: +44 (0)114 271 3687.
E-mail address: j.w.fenner@sheffield.ac.uk (J. Fenner).

1120-1797/$ – see front matter © 2014 Associazione Italiana di Fisica Medica. Published by Elsevier Ltd. All rights reserved.
http://dx.doi.org/10.1016/j.ejmp.2013.12.002

[14–17]. The diagnostic reporting of scans can be time consuming for the radiologist (since the process involves the analysis of many images), so the technique is not without cost-benefit implications. Nonetheless its diagnostic value appears beyond reproach in the hands of a specialist [14], but arguably this deserves qualification since diagnosis by such methods may only be tractable in advanced stages of disease [12].

We exploit image registration as a tool to quantify anatomical movement within diagnostic sequences of images and hypothesise that movement anomalies are diagnostic of abnormalities in underlying physical structures (e.g. adhesions). We postulate that this may support disease localisation and accelerate diagnosis. This was explored using a variety of models (*in vitro*, *in silico*) and the outcomes quantitatively evaluated. Ultimately this led to application in a clinical example, and results are presented.

The participants supporting the development of this technique covered a wide range of experience and expertise, with early trials involving clinicians (radiologists, gastroenterologists, surgeons) as well as more technical participants from medical physics/imaging backgrounds. The models presented here tend to have an abdominal bias because our interest is the motion of abdominal anatomy for detection of adhesions, but this is not inherent to the method. It can readily be extended to other domains. This paper describes development of techniques that were used to explore issues relevant to the hypothesis, ultimately yielding a proof-of-concept tool that demonstrates potential in clinical practice.

Materials and methods

The diagnostic technique presented here [18] relies on image processing support to aid the tracking of characteristic features within a temporal sequence of images. Initially a simulated environment was constructed to emulate the diagnostic challenge and exercise the software algorithms. This was a vehicle for training the user and developing/quantifying the image processing aid. This was followed by a progression of increasingly demanding diagnostic scenarios, eventually leading to application in a clinical example. The sequence of technical developments is reported below.

Experiment 1: a physical model and a preliminary qualitative study

As with many dynamic, diagnostic imaging sequences, diagnosis of adhesions requires interpretation of motions captured in a 2D plane, and our interest is identification of subtle changes to that movement (introduced by small defects) that may be masked by the complexities of the anatomical image. Hence a simple test environment was constructed for proof of concept purposes, built around a 2D mechanical analogue (see Fig. 1), designed to encapsulate the principles of diagnosis through identification of disturbed movement. It also loosely acknowledges the displacement of the diaphragm at the periphery of the abdominal cavity. The observer was required to infer the presence of an underlying structural abnormality, diagnosed from anomalous movement of an overlying image. Performance with and without image processing permitted the relative effectiveness of the image processing support to be assessed.

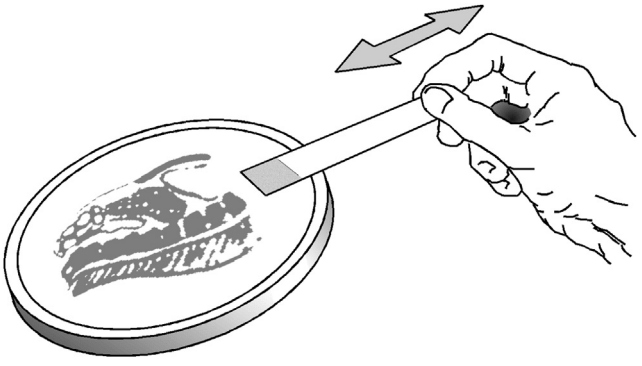

Figure 1. Physical test rig: An image was drawn onto an elastic sheet. This was tensioned over a circular frame, and distorted by pulling an attached piece of tape.

Physical model

The physical model employed an opaque and lightly tensioned elastic sheet overlaid on a sewing ring of 15 cm diameter, with an image drawn on its surface (Fig. 1). The end of a length of tape was attached near the periphery, which could be pulled to deform the sheet. A rig was constructed to enable repeated pulling and relaxation (~1 Hz) of the diaphragmatic region of the image, causing movement that distorted all parts of the image in a reproducible manner. The whole cycle was captured as a digital video using a camera operating at 15 fps, providing a baseline animation that represented 'normal' movement. In order to introduce subtle, localised disturbance to the motion, a small, square, inelastic sticky sheet (1 cm^2) was securely attached near the centre of the image on the reverse side of the elastic material that was fixed to the sewing ring (i.e. it was invisible to the camera). Therefore, when the tensioning tape was pulled to distort the elastic image within the sewing ring, the inelastic defect suffered a displacement but moderated the local elastic strain (and the implicit motion of the overlying image). The stretching cycle was again captured as a digital animation. An observer was blinded to the presence/absence of the defect, so that when presented with the video footage, he/she was required to analyse it to…

- Identify if the motion of the image was 'normal' (no defect present) or 'abnormal' (sticky tape defect present)
- Localise the defect in those cases in which it was judged to be present.

The inelastic tape responsible for the defect could be placed in different locations to generate a gamut of movement restrictions. Analysis of the video images by the observer was performed with and without image processing assistance to ascertain its effectiveness in assisting with the identification of subtle disturbances concealed within the movements of the image. Two levels of image complexity were employed separately in this experiment, the first utilising a simple image (square grid) and the second, a cartoon representation of a sagittal abdominal MRI slice (medium complexity image – Fig. 2).

Image processing

Our image processing methodology used the registration technique developed by Barber and Hose [19], which computes a mathematical transformation (non-affine) that maps a reference image to another similar image. This is ideal for quantifying movement within a collection of similar images that constitute a dynamic sequence. The mapping has its basis in a numerical variational methodology that computes a continuous vector field. This describes the local displacement needed to map every visual structure in a source image to an equivalent visual structure in a target image. Subsequent analysis of the vector field and appropriate visualisation can reveal the motion of the visual structures contained within the field of view, and yield characteristic signatures that are indicative of perturbations to that movement. Our preferred method of visualisation reduces the vector data to contour maps of vector magnitude (see Fig. 2). Numerous other data presentation strategies are possible, but our chosen method was

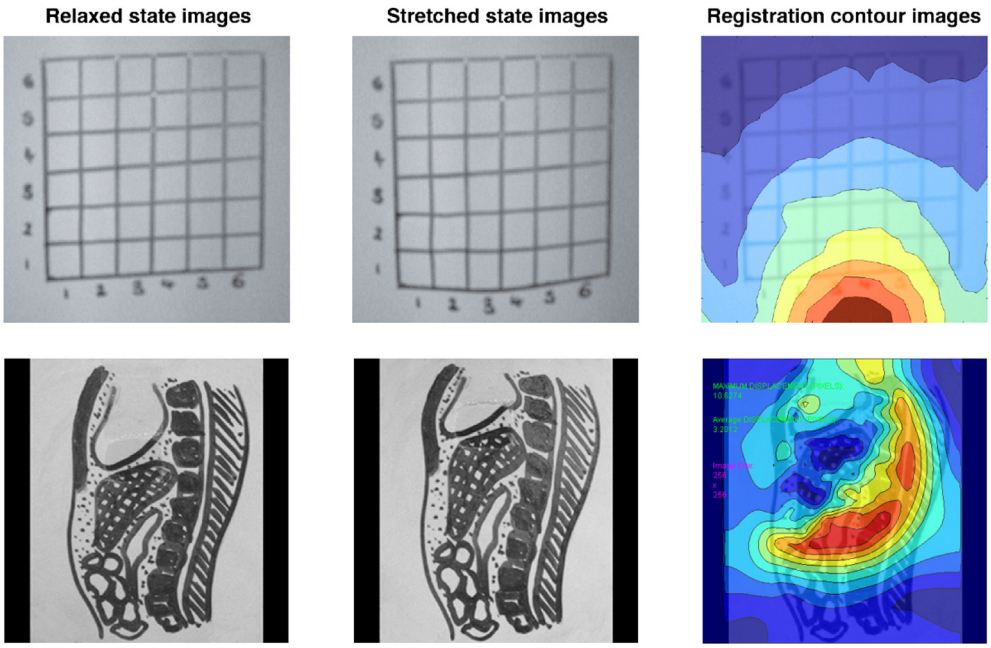

Figure 2. Images from the physical experiment. The stiffness anomaly is present in square (2,2) of the images in the top row, and approximately in the centre of the cartoon images in the bottom row. Disruption to the movement contours computed by the image processing correlates with the presence/absence/location of the hidden inelastic defect.

simple to compute and proved to be readily interpretable by a radiologist.

The ShIRT (Sheffield Image Registration Toolkit) implementation of the algorithm [19] was used for this study, and although it offers many user-configurable options, we chose to operate it according to its default settings. It solved the most demanding image registration tasks with a smoothing parameter (λ) of approximately 30, and a node spacing of 4 pixels. Compute time for 512 × 512 pixel images was about 5 s on a modern laptop equipped with an Intel i3, 2.2 GHz processor and 8 GB RAM.

Experiment 2: an in silico model with fixed and moving defects

Limitations of the physical model led to extension of the technique through virtualisation and replication of the physical model *in silico*. In principle, an *in silico* simulation can capture all the features of the physical model, but also offers numerous advantages (e.g. improved reproducibility of experimental conditions). The *in silico* model was constructed using a 2-dimensional Finite Element (FE) simulation of the elastic sheet, with a facility to stiffen areas of the FE mesh to emulate attachment of the inelastic defect present in the physical model. Furthermore, the simulation was designed to accommodate a superimposed image, which was distorted in accordance with the underlying mesh (similar to u, v texture mapping techniques encountered in computer graphics [20]). A regular mesh consisting of square (4-node) elements was used to formulate the underlying elastic fabric on which the image was placed. In order to minimise artefactual behaviour that might emerge from such an unnaturally perfect system, the mesh element stiffnesses were randomly varied up to ~30% about the mean from

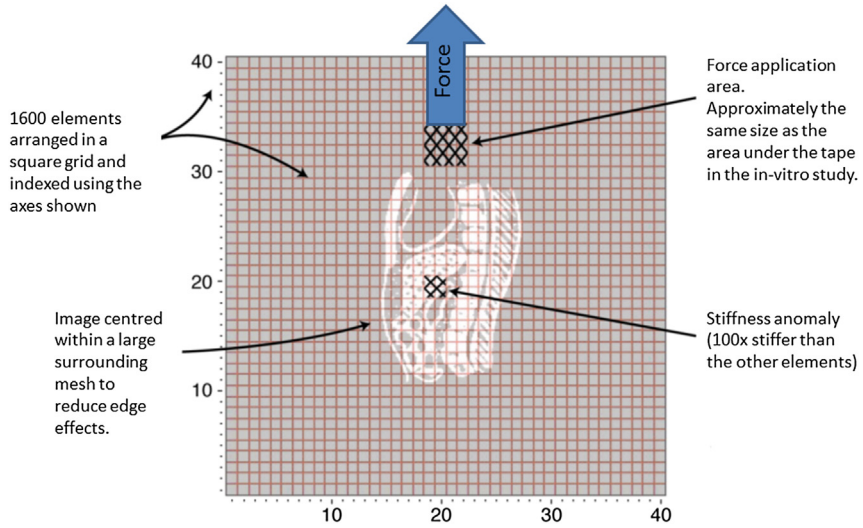

Figure 3. The *in silico* model consists of a finite element mesh of 40 × 40 elements with an overlying image placed at its centre. Application of an incremental force distorts the mesh and overlying image. Successive frames are compiled into an animation of 40 frames that runs at 15 frames per second.

element to element. Average properties of the mesh were set to achieve similar behaviour to the physical model, and a small, localised area of higher stiffness (100 times stiffer) was introduced to simulate the presence of a defect. Once created, the mesh was subjected to the forces responsible for the stretching of the elastic sheet and the new nodal positions computed (Fig. 3). The distorted mesh was used to derive a distorted image (which was captured as a video frame), and this was repeated for incrementally varying displacements to create a multi-frame animation.

Three levels of image complexity were modelled using the *in silico* system (simple, medium and complex; Fig. 4). The simple and medium images were high resolution, digitally scanned copies of the images used in the physical experiment. The complex image was a real sagittal slice taken from an MRI scan of a volunteer. These provided the source images for the *in silico* experiments, thus enabling quantification of an observer's ability to identify the presence/absence of an underlying structural defect, inferred from movement anomalies of the overlying image.

Several exercises were used to determine the sensitivity of an observer to defects, with and without image processing assistance. The technical protocol for generating data relating to the test is reported below:

Technical protocol:

1) For each level of image complexity (simple, medium, complex) 160 animations were formed (i.e. $160 \times 3 = 480$ animations in total). Half of the animations featured a defect and the other half did not.
2) In each case, the mesh element noise was recomputed and reapplied using a different random number seed. Appropriate distorted images were computed anew and animations compiled.
3) The animations were randomised and then presented consecutively to the observer (who was blinded to the sequence).

Diagnostic effectiveness was characterised using the observer protocol described below.

Observer protocol:

1) When presented with each animation the observer was asked to identify whether a defect was present or not, and his/her response was recorded.
2) With each response, the observer was required to quantify the certainty of his/her observation according to a 7-point scale:
   - I am absolutely sure a defect is present
   - I suspect a defect is probably present
   - I think a defect is possibly present
   - I have no idea if a defect is present or absent. This is a pure guess.
   - I think a defect is possibly absent
   - I suspect a defect is probably absent
   - I am absolutely sure a defect is absent
3) If a defect was deemed to be present, the observer was required to localise its position with reference to the coordinates of a 3×3 grid.
4) For purposes of comparison, the exercise was repeated in its entirety with and without the use of the image registration tool.
5) Data was collated and a measure of diagnostic performance obtained using ROC methods [21,22].

The performance of four observers is reported in this study, providing the final ROC data as presented in Fig. 5. This involved both technical and inexperienced clinical observers; ages ranged from early-twenties to mid-forties. Each was required to engage in a training session prior to the study, to prepare him/herself and become familiar with the diagnostic concepts and challenges involved.

Experiment 3: clinical application

Having gained considerable experience with increasingly demanding but simulated diagnostic scenarios, the image processing methodology was finally exercised in the context of patient data, for preliminary clinical evaluation. This applied the skills acquired in the simulated environment to real clinical images. The clinical condition chosen for this demonstration was Encapsulating Peritoneal Sclerosis (EPS), which is an extreme manifestation of adhesions, frequently associated with long term exposure to Peritoneal Dialysis. Currently no effective mechanism for its early diagnosis exists, except in the often fatal late stages of the disease in which biomarkers reveal loss of ultrafiltration. Peritoneal thickening may be evident with Computed Tomography [4,23].

Clinical images were obtained from two different hospital sites. EPS patient data was obtained from the Wellcome Trust Clinical Research Facility in Manchester (UK), and for purposes of comparison, a control set of healthy volunteer data was available from Rotherham District General Hospital (UK). The scan protocol included a series of sagittal and transverse acquisitions, encompassing the full abdomen and pelvis. In both cases (healthy volunteers and EPS patients), the MR imaging sequence used a TRUE

Figure 4. Three image types were used in the *in silico* study, designated left-to-right as, simple, medium and complex.

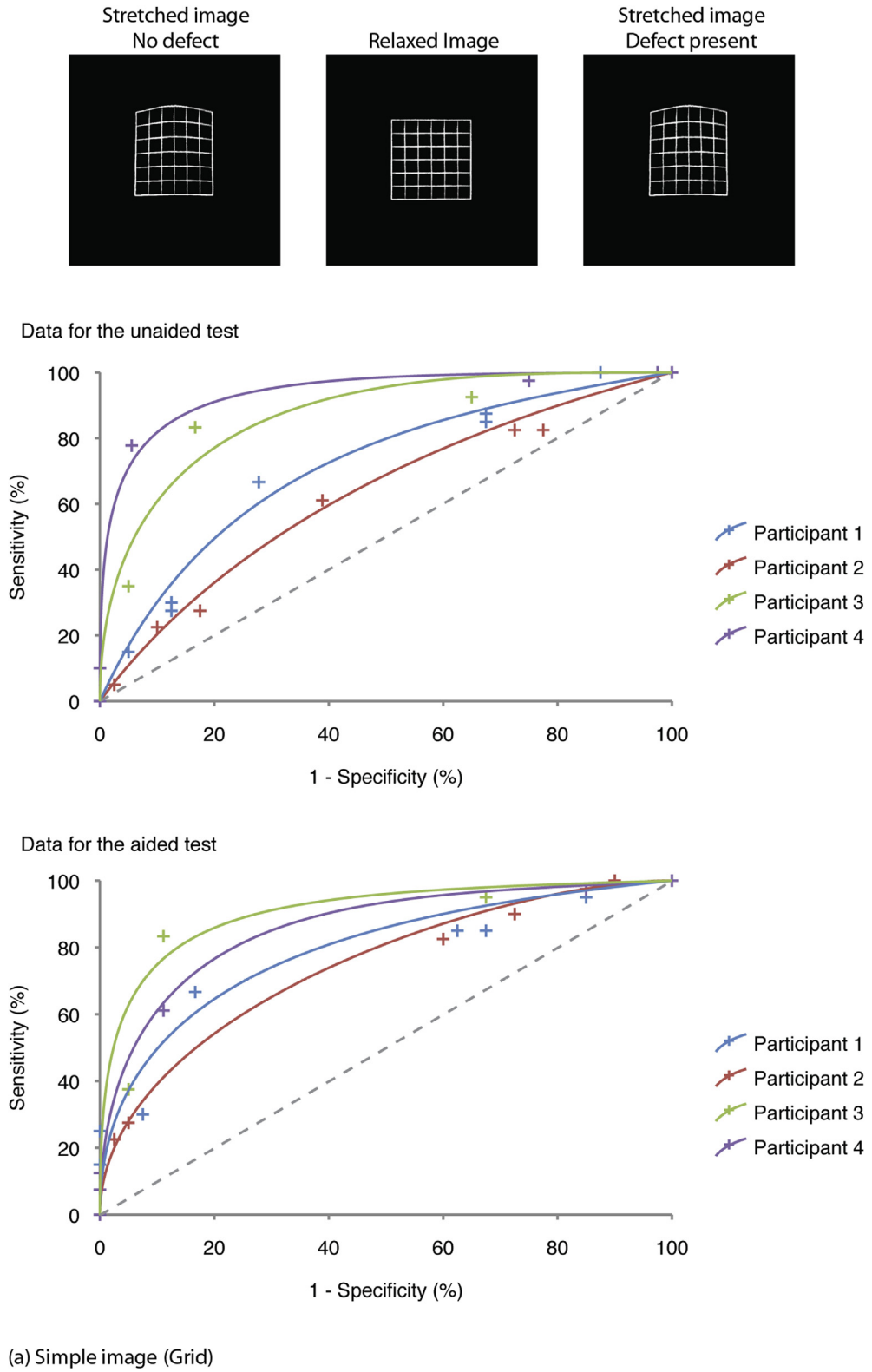

Figure 5. Best fit by eye, ROC curves for 4 participants (*in silico* trials) – (a) simple image (b) medium complexity image and (c) complex image. Unaided (i.e. no image processing support) and aided curves are shown. The line of no discrimination is displayed as the dashed line. Notably improved diagnostic performance is apparent with image processing support in (b) and (c), with mean area under curve (AUC) values improving from 0.67 ± 0.02 to 0.87 ± 0.02.

FISP (true-fast imaging with steadystate precession) acquisition, with each participant recumbent in the supine position. Sagittal slices revealed the anatomy, from the middle of the descending colon to the middle of the ascending colon, with the superior-inferior field of view (FOV) large enough to include the symphysis pubis and the diaphragm where possible. Successive slices were available, with a 10 mm gap introduced between each slice in both orientations. The acquisition covered the respiratory

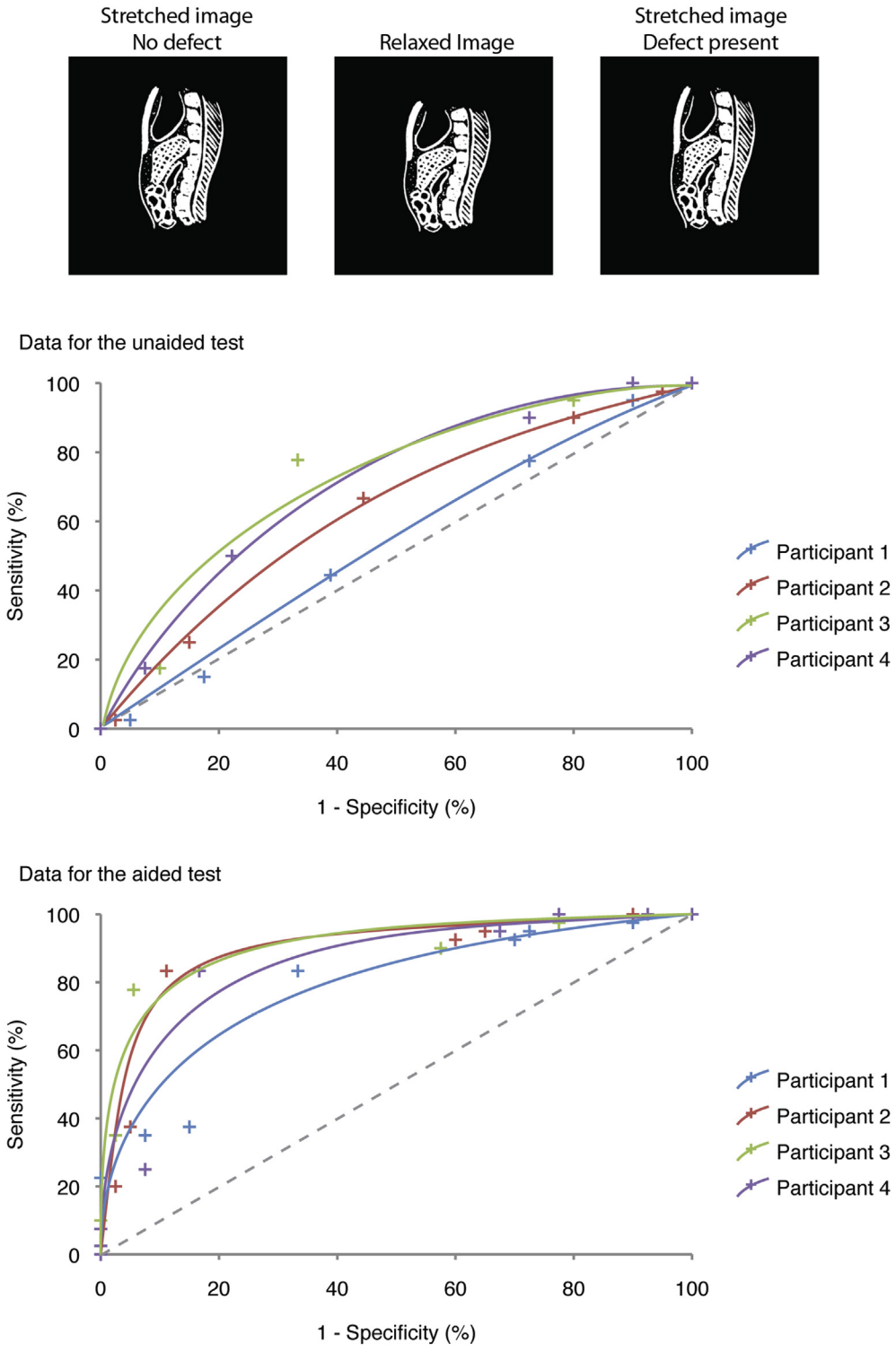

Figure 5. (*continued*).

cycle to ensure that the complete range of movements was recorded. The average breathing cycle was assumed to take approximately 3 s, approximating 20 Cycles Per Minute (CPM). This is more rapid than the normal adult autonomic breathing rate (typically 12CPM), but participation in the MR scan is observed to shorten the cycle length, perhaps because of stress or the slightly unnatural pose required of the participant. A dynamic sequence composed of 15 stills taken in rapid succession

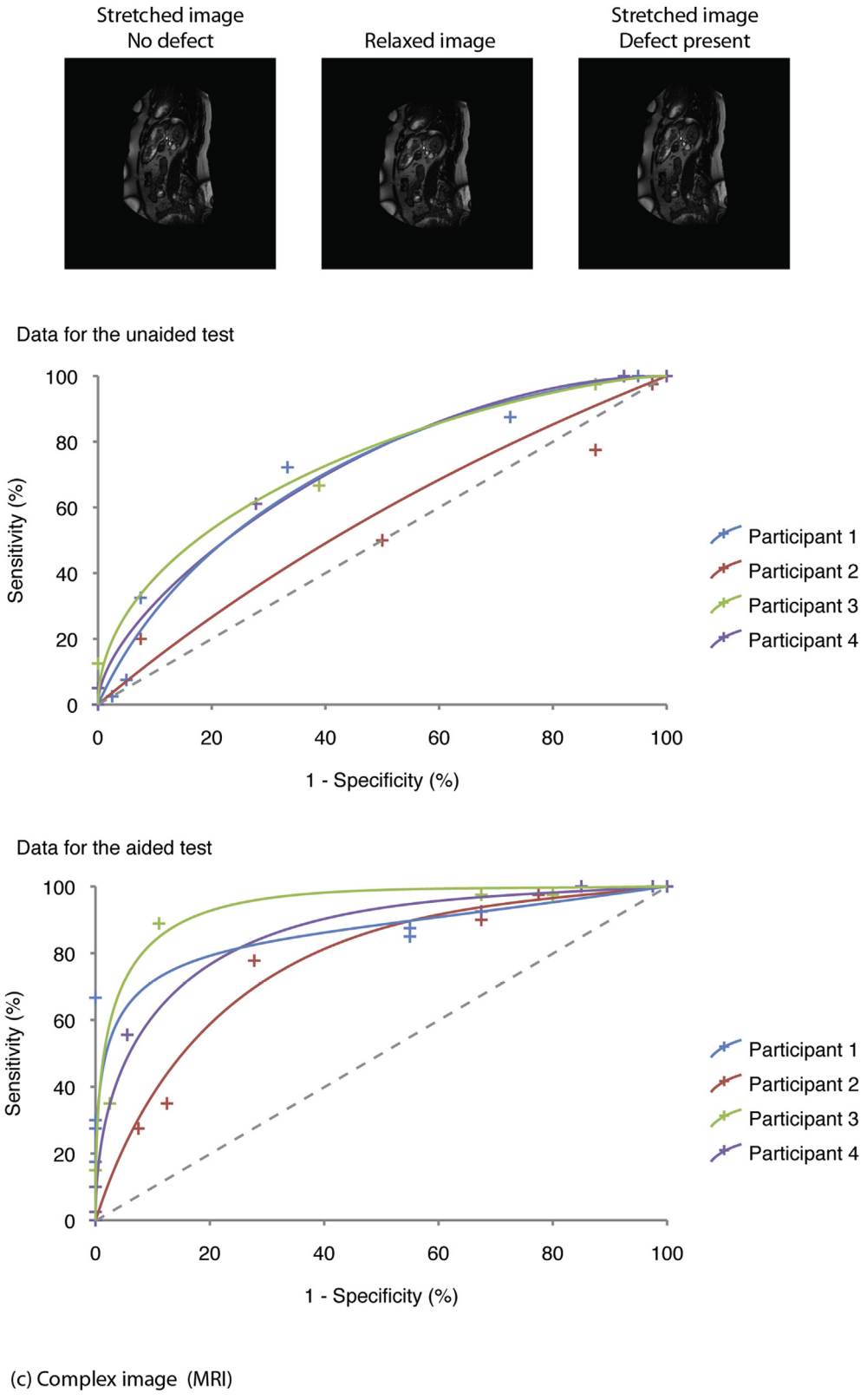

Figure 5. (*continued*).

covered a 12 s period. This ensured that the maximum excursions of the volunteer respiratory cycle were captured. Consequently, at each slice position, 15 images were present, accommodating anatomy in which the participant had been asked to 'breathe normally' as well as 'bear down' (as if going to the toilet – in lieu of a Valsalva manoeuvre [24]).

Participants in this study were ethically selected, on the basis of availability and consent. The healthy volunteer of Fig. 6 (left image)

was a fit, 21-year old male who had no previous abdominal surgical history and was assumed to be adhesion free. In contrast, the male patient volunteer with EPS shown in the adjacent image on the right was aged 40 and quite ill. He had been on peritoneal dialysis for 84 months and developed EPS following a transfer to haemodialysis. Peritonectomy and adhesiolysis were used to relieve the condition, but he presented with severe gastrointestinal symptoms and weight loss 1 year later. The patient was suspected of recurrent EPS which was subsequently confirmed surgically. In both cases the resultant series of images were viewed using the standard MR system cine software. Images of largest gross movement within each sagittal slice were hand-picked as pairs for the registration process. This approach was used to select both the EPS and the healthy volunteer data, creating image pairs that (in principle) captured the extremes of diaphragmatic motion. Once selected, the image pairs were registered to one another and the results post-processed to produce contour plots as described for the simulated data.

Statistics

These experiments were designed to quantify the degree to which the image processing tool can augment the identification of subtle motion-based disturbances that might be precipitated by the presence of a structural defect. In particular, the *in silico* experiments present two classes of movement, one in which the motion of the image reflects the unconstrained response to the stretching of the underlying fabric on which it is placed, whilst the other introduces a local stiffness that moderates the mechanical displacements of the underlying fabric and thereby locally disturbs the movement of the image. The challenge faced by the observer is to diagnose the presence or absence of the defect by simple observation of the distorting image. The computer presents a randomised selection of movies, each of which may or may not contain a defect, and for every movie that was viewed, the observer was required to conclude whether he/she believed the anomaly to be present or absent (i.e. diagnosis). For the *in silico* experiments, a trial involved the analysis of a statistically adequate number of movies (160) with every diagnostic outcome compared with the true status of defect presence/absence/locale in each case. This provided data for a truth table that clarified important diagnostic quantities, such as True Positive Rate, False Positive Rate. The facility for the observer to record the certainty of their response (ranging from completely uncertain to absolutely certain, based on a 7-point scale) enabled the role of diagnostic thresholds to be explored. Through the plotting of an ROC curve, the relative diagnostic power of each of the assessment methods was quantified. Hence diagnostic performance was characterised and compared for a range of image complexities (simple, medium and complex), with and without the use of the image processing tool.

No metrics were developed for the clinical exercise, except to identify a correlation between the output of the image processing and the EPS status of our volunteer patient, as confirmed by surgery.

Results

These results present data from the initial practical *in vitro* work that was undertaken as well as the more extensive assessment using the *in silico* testing environment. Finally, outcomes from the clinical scenario are described too.

Results for experiment 1: physical model and in-vitro analysis

The physical model of experiment 1 produced data (see Table 1) that characterised an observer's ability to diagnose the location of a

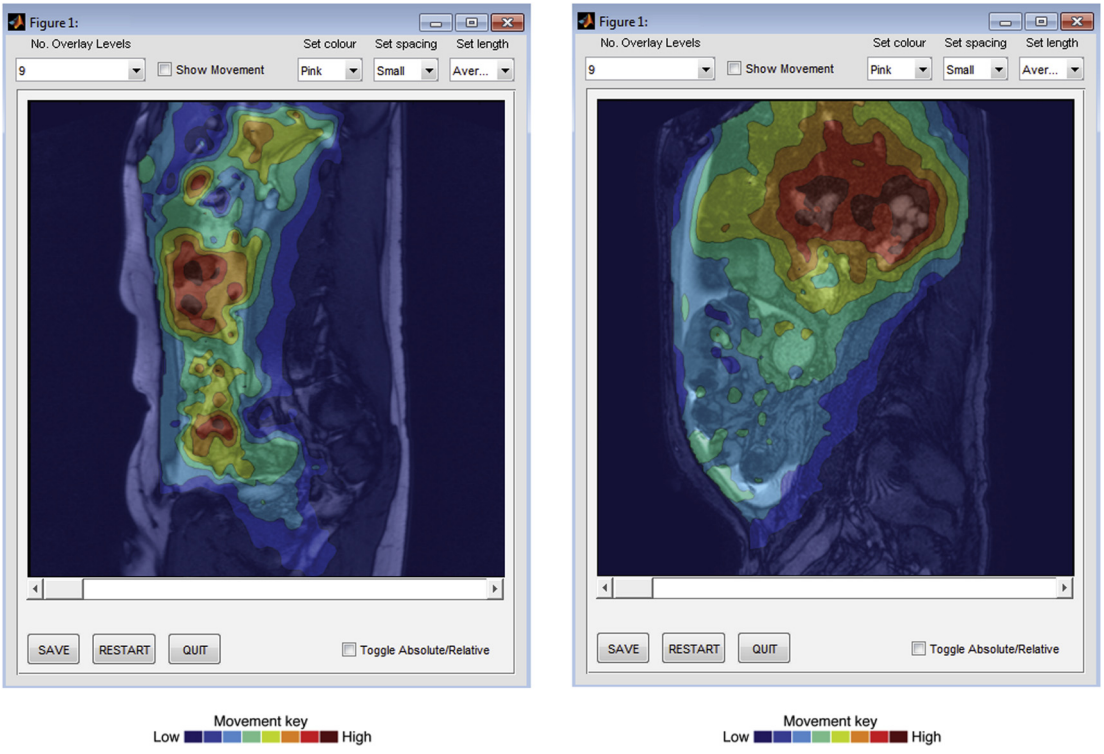

Figure 6. The example on the left depicts the movement contours associated with a healthy volunteer and indicates diffuse movement of the internal organs throughout the abdominal cavity. In contrast, image data on the right indicates a block of localised movement in the vicinity of the diaphragm. This is consistent with a pathology (EPS) that wraps the organs in a stiff and strangulating cocoon of visceral tissue.

hidden stiffness anomaly placed underneath an image on a deforming elastic sheet. The exercise provided semi-quantitative confirmation of the following:

- In the case of the (simple) square grid, visual analysis of the distorting image enabled the observer to infer the locations of underlying structural abnormalities. No image processing support was necessary for effective 'diagnosis'.
- Visual analysis of the moving cartoon image of anatomy was generally sufficient to localise an underlying structural abnormality, but experience indicated that this was augmented when image processing support was available. Note that the 'augmentation' was not in respect of improved diagnostic statistics, rather the image processing provided supporting information that reassured the observers, giving confidence in their 'diagnosis'. Interestingly, observers reported that they found the image processing to be largely irrelevant in the case of the simple grid.

Examples of the analyses obtained with these images are shown in Fig. 2. This evaluation confirmed that anomalies in the movement of an overlying image can be related to abnormalities in the underlying structure (e.g. adhesions). However, restrictive limitations of the method provided impetus for its replication *in silico*, yielding an experiment with much more tightly controlled testing conditions.

Results for experiment 2: in silico model with fixed and moving defect

The results of the *in silico* experiments provided quantitative information about observer and image processing performance that echoed the qualitative results of the physical experiment above, but also extended the technique to include an MRI image. The *in silico* data has been compiled and distilled as ROC curves, as illustrated in Fig. 5a–c. ROC plots refer to the following trials:

Table 1
Results of an *in vitro* experiment requiring localisation of anomaly stiffness. Coordinates relate to the grid location of the stiffness anomaly. No image processing was used in this example. Observer errors are present, but in general they tend to be small. The results confirm the practicality of identifying structural abnormalities from anomalous movement of an overlying image.

Case number	Predicted coordinates	Actual coordinates	Correct localisation (Y/N)	Localisation Error (predicted − actual)
1	(5,4)	(5,4)	Y	
2	(2,4)	(2,4)	Y	
3	(2,2)	(2,2)	Y	
4	(2,5)	(2,6)	N	(0,1)
5	(5,3)	(2,6)	N	(−3,3)
6	(5,4)	(4,4)	N	(−1,0)
7	(3,3)	(5,4)	N	(2,1)
8	(4,1)	(4,1)	Y	
9	(3,4)	(3,5)	N	(0,1)
10	(4,6)	(5,5)	N	(1,−1)
11	(3,2)	(3,1)	N	(0,−1)
12	(1,4)	(1,4)	Y	
13	(4,1)	(4,1)	Y	
14	(2,3)	(2,3)	Y	
15	(4,2)	(4,2)	Y	
16	(4,3)	(4,3)	Y	
17	(5,5)	(2,6)	N	(−3,1)
18	(2,4)	(2,4)	Y	
19	(6,4)	(6,4)	Y	
20	(1,1)	(4,6)	N	(3,5)
Correct localisations				11
Incorrect localisations				9

Table 2
These *in silico* results indicate that the time required to make a diagnosis of the more complex images can decrease if the observer is aided by the image processing software.

	Time taken (s)	
	Unaided ± 1 SD	Aided ± 1 SD
Grid	83.4 ± 20.8	90.5 ± 30.4
Cartoon	92.1 ± 35.8	45.9 ± 23.5
cMRI	99.8 ± 56.3	80.43 ± 61.0

Fig. 5a:
- simple image; unaided, no image processing support
- simple image; image processing used to aid defect detection

Fig. 5b:
- cartoon image; unaided, no image processing support
- cartoon image; image processing used to aid defect detection

Fig. 5c:
- MRI image; unaided, no image processing support
- MRI image; image processing used to aid defect detection

The plots present diagnostic performance for 4 observers in each of the 6 trials (i.e. image processing present/absent with simple, medium and complex images). Localisation errors were generally small and comparable to those found in the physical model (Table 1). In respect of the presence/absence of a defect, note that there is little difference – unaided or aided by image processing – in the case of the simple grid image (Fig. 5a); the area under the ROC curve (AUC) changes from 0.80 ± 0.14 to 0.82 ± 0.07. This contrasts with significantly improved performance provided by image processing support in the cases of the more complex cartoon and MRI images (Fig 5b,c). The cartoon AUC changes from 0.65 ± 0.09 (unaided) to 0.87 ± 0.06 (aided), and the MRI AUC changes from 0.68 ± 0.08 (unaided) to 0.87 ± 0.07 (aided). Table 2 completes the data by indicating average times taken to reach a diagnostic decision for each image type.

Results for experiment 3: clinical application

Image registration contour data for two clinical examples is presented in Fig. 6. The contours indicate that abdominal movement of healthy individuals is dispersed throughout the abdominal cavity. Zones of equally high movement are seen throughout the abdomen, and diffuse motion is readily observed in the moving cine-MRI footage. In contrast, the EPS patient data indicates that movement is concentrated towards the top (superior) of the abdominal cavity. The small bowel appears to impede dispersion of the movement, perhaps due to the elevated stiffness of the EPS cocoon, as confirmed by surgical investigation.

Discussion

The developments described in this paper have exercised the registration-based image-processing technique in pursuit of augmented diagnosis of disturbances to healthy abdominal movement. Our hypothesis is that anomalous movement signatures can reveal underlying structural defects. Diagnosis of the more complex images (with or without image processing support) proved predictably difficult, confirming that anomalous movement can easily be masked by images containing complex and distracting features. However, the registration-based image processing method proved effective in the *in silico* diagnostic tests, supporting developments that led to a very limited but encouraging demonstration in the clinical domain.

Experimental observations

The physical experiment provided initial semi-quantitative data that supported our hypothesis (i.e. image registration can be used to quantify anatomical movement, with potential to reveal pathological anomalies) and encouraged further developments. A more quantitative assessment using the physical model was attempted but it could not sustain the number of repeated measurements required. (For instance the adhesive tape lost its stickiness, the elastic sheet perished, accuracy of placement of the defect was limited, creation of an imaging sequence of reproducible and adequate quality was very time consuming in each case etc.). It was limitations such as these that prompted redesign of the experiment as a whole (*in silico*). Nonetheless, this initial assessment provided some intriguing data. It confirmed that underlying structural abnormalities can be inferred from the anomalous movement of an overlying image, and yet it also raised questions about the effectiveness of image processing in relation to image complexity. These results were replicated by the *in silico* results (e.g. Fig. 5a), illustrating the efficacy with which an unassisted observer can localise a defect when working with the square grid image. Diagnosis was not improved with the support of image processing and it rapidly became clear that in this case the image processing tool contributed little to diagnosis. However, in the incrementally more complex cartoon image, the diagnostic task was aided by the use of the software. With hindsight, it seems likely that reduced complexity as represented by a highly ordered image (i.e. grid) is of benefit to the human observer, whose eye is naturally drawn to anomalies in the simple, quantifiable regularity of the shapes (straight edges, right-angled corners, symmetry, similar squares that can be compared with each other etc). Here, image processing is not required for effective diagnosis. In contrast, the cartoon image offers little in the way of such features and therefore human strategies for quantification are much more difficult. In this case, application of the image processing/visualisation reduces the information content to provide an alternative image (stripped of its 'anatomical' complexity) by simply displaying displacement contours. This provides a pattern (i.e. contour map showing bands of equal movement) that is much more amenable to human quantification and provides an identifiable signature indicative of an anomaly. In spite of this, the ability to accurately localise a defect was less than perfect. The diagnostic signature was sufficient to alert the suspicions of the observer to the presence of a defect, but in general, localisation rarely improved upon the physical grid results reported in Table 1.

These exercises generated strong resonances with the experiences of radiology experts present in our research team. They seemed to exemplify many of the dilemmas associated with diagnosis of movement signatures in the clinical domain. In particular, careful analysis of the moving images was required, with due consideration of numerous additional factors before a diagnosis could be given (e.g. corroborating evidence from other parts of the image). The outcome of these evaluations indicated that certain classes of image (e.g. regular grids) favoured diagnosis with the unaided human eye, whereas the use of more complex images proved much more challenging and vindicated use of the software for detection of a defect.

Training

The training of an observer in preparation for any of the diagnostic evaluation exercises was an important feature of our experimental protocol. This comprised a 30 min session involving the observer and an expert, with much discussion and interactive evaluation of a sequence of training scans typical of the types to be encountered in the test. This helped the trainee to identify visual cues and establish his/her own ruleset on which to base diagnosis. Feedback from participants identified that the majority of observers largely ignored the information provided by the image processing in the case of the simple images of the stretched square grid - the image processing data was deemed to be 'distracting' and 'unhelpful'. Conversely, the challenge of identifying an adhesion within the group of animations involving complex MRI images meant that few observers took the effort to analyse multiple frames of the cine sequences by eye if image processing data was available, since the latter appeared to communicate most of the important information pertinent to diagnosis.

Clinical context

The clinical motivation for this work comes from a pathology – abdominal adhesions - that is difficult to identify and is typically a diagnosis of exclusion. The use of diagnostic imaging and image processing to augment the efficacy of diagnosis is a common theme in clinical imaging. Traditional image processing approaches attempt to isolate organs by segmentation [25], and this can be an effective method for tracking their motion but is very challenging in the abdominal domain. The application of image registration offers an alternative approach [26,27], since segmentation is not required. Image registration is employed as a technique for characterising movement, mathematically comparing two images to produce a vector map of pixel displacements that maps one image to the next. Selected images in the cine-MRI sequence are registered, the vector data analysed and the results presented to the radiologist (e.g. visualised) for interpretation. The limited clinical application of the software to the aggressive, adhesive pathology of EPS has demonstrated the feasibility of this approach in this instance. A more comprehensive clinical assessment is beyond the scope of this paper, since the work presented here is concerned with justifying the methodology. Nonetheless, more extensive trials are required before it might be considered suitable for wider clinical deployment, and the interested reader is referred to the work of Wright et al. [28] for further evidence of its clinical application. A pilot study is also underway, funded by KRUK.[1]

A broader perspective

The advent of imaging and digital imaging in particular, has provided a technology that complements qualitative vision with quantitative analysis, and the application of image processing extends the utility of both even further. Our application exploits the acuteness of the radiologist's eye and marries it with the quantitative capabilities of image registration for diagnostic benefit. With respect to clinical imaging and diagnosis, issues of sensitivity and specificity are of importance, and the use of ROC analysis in this case has shown it to be effective in driving the development of tools designed to optimise diagnosis of adhesions, with implications for patient management.

Conclusion

This paper reports a method for characterising diagnostic features of a temporal image sequence of complex anatomy in the context of diagnosing abdominal adhesions. This is a goal that benefits from an effective testing environment and both the image processing tool and environment have been described. Together they have delivered a potentially relevant clinical tool, based on a

[1] Kidney Research UK – http://www.kidneyresearchuk.org.

movement model coupled with an image processing technique (image registration) and visualisation. These have been optimised to expose subtle disturbances to anatomical movement, indicative of underlying structural abnormality. Quantitative ROC methods have been used to demonstrate a significant degree of diagnostic augmentation.

Acknowledgements

The authors wish to express their gratitude to BRET (Bardhan Research and Education Trust of Rotherham Limited) and the EPSRC (Engineering and Physical Sciences Research Council, UK) for the funding of this research. We are also pleased to acknowledge the contribution of the numerous observers who patiently analysed and 'diagnosed' many images for the purposes of this work. Finally we are grateful to Kidney Research UK for its support of continuing developments.

References

[1] Vrijland WW, Jeekel J, Geldorp HJ, Swank DJ, Bonjer HJ. Abdominal adhesions: intestinal obstruction, pain, and infertility. Surg Endosc 2003;17(7):1017–22.
[2] Ellis H, Moran BJ, Thompson JN, Parker MC, Wilson MS, Menzies D, et al. Adhesion-related hospital readmissions after abdominal and pelvic surgery: a retrospective cohort study. Lancet 1999;353(9163):1476–80.
[3] Boland GM, Weigel RJ. Formation and prevention of postoperative abdominal adhesions. J Surg Res 2006;132(1):3–12.
[4] Kawanishi H. The pathogenesis and therapeutic option of encapsulating peritoneal sclerosis. Int J Artif Organs 2005;28(2):150–5.
[5] Langer SG, Ramthun S, Bender C. Introduction to digital medical image management: departmental concerns. Am J Roentgenol 2012;198(4):746–53.
[6] Hansmann J, Eichholz J. Radiological diagnostics of the small bowel. Radiologe 2012;52(9):849–66.
[7] Barnett RE, Younga J, Harris B, Keskey RC, Nisbett D, Perry J, et al. Accuracy of computed tomography in small bowel obstruction. Am Surg 2013;79(6):641–3.
[8] Osada H, Watanabe W, Ohno H, Okada T, Yanagita H, Takahashi T, et al. Multidetector CT appearance of adhesion-induced small bowel obstructions: matted adhesions versus single adhesive bands. Jpn J Radiol 2012;30(9):706–12.
[9] Shakil O, Zafar SN, Zia-ur-Rehman Saleem S, Khan R, Pal KM. The role of computed tomography for identifying mechanical bowel obstruction in a Pakistani population. J Pak Med Assoc 2011;61(9):871–4.
[10] Jackson PG, Raiji MT. Evaluation and management of intestinal obstruction. Am Fam Physician 2011;82(2):159–65.
[11] Minordi LM, Vecchioli A, Mirk P, Bonomo L. CT enterography with polyethylene glycol solution vs CT enteroclysis in small bowel disease. Br J Radiol 2011;84(998):112–9.
[12] Stuart S. Can detection of changes in the motion of abdominal contents using "cine" MRI help in the management of encapsulating peritoneal sclerosis? Perit Dial Int 2011;31:267–8.
[13] Vimercati A, Achilarre MT, Scardapane A, Lorusso F, Ceci O, Mangiatordi G, et al. Accuracy of transvaginal sonography and contrast-enhanced magnetic resonance-colonography for the presurgical staging of deep infiltrating endometriosis. Ultrasound Obstet Gynecol 2012;40(5):592–603.
[14] Lienemann A, Sprenger D, Steitz HO, Korell M, Reiser M. Detection and mapping of intraabdominal adhesions by using functional cine MR imaging: preliminary results. Radiology 2000;217(2):421–5.
[15] Lang RA, Buhmann S, Hopman A, Steitz HO, Lienemann A, Reiser MF, et al. Cine-MRI detection of intraabdominal adhesions: correlation with intraoperative findings in 89 consecutive cases. Surg Endosc 2008;22(11):2455–61.
[16] Caprini JA, Arcelus JA, Swanson J, Coats R, Hoffman K, Brosnan JJ, et al. The ultrasonic localization of abdominal wall adhesions. Surg Endosc 1995;9(3):283–5.
[17] Mussack T, Fischer T, Ladurner R, Gangkofer A, Bensler S, Hallfeldt KK, et al. Cine magnetic resonance imaging vs high-resolution ultrasonography for detection of adhesions after laparoscopic and open incisional hernia repair: a matched pair pilot analysis. Surg Endosc 2005;19(12):1538–43.
[18] Wright B. The use of image registration to aid identification of abdominal adhesions. PhD thesis. University of Sheffield; 2011.
[19] Barber DC, Hose DR. Automatic segmentation of medical images using image registration: diagnostic and simulation applications. J Med Eng Technol 2005;29(2):53–63.
[20] Foley JD, van Dam A, Feiner SK, Hughes JF. Computer graphics: principles and practice. 2nd ed. Addison Wesley; 1995.
[21] Murphy JM, Berwick DM, Weinstein MC, Borus JF, Budman SH,Klerman GL. Performance of screening and diagnostic tests: application of receiver operating characteristic analysis. Arch Gen Psychiatry 1987;44(6):550–5.
[22] Obuchowski NA. Receiver operating characteristic curves and their use in radiology. Radiology 2003;229(1):3–8.
[23] Tarzi RM, Lim A, Moser S, Ahmad S, George A, Balasubramaniam G, et al. Assessing the validity of an abdominal CT scoring system in the diagnosis of encapsulating peritoneal sclerosis. Clin J Am Soc Nephrol 2008;3(6):1702–10.
[24] Nishimura RA, Tajik J. The Valsalva maneuver and response revisited. Mayo clinic proceedings. Mayo Clinic 1986 (March);61(3):211–7.
[25] Sharma N, Aggarwal LM. Automated medical image segmentation techniques. J Med Phys 2010;35(1):3–14.
[26] Modersitzki J. Numerical methods for image registration. Published by Oxford University Press; 2004. ISBN 978-0-19-852841-8.
[27] Hill DL, Batchelor PG, Holden M, Hawkes DJ. Medical image registration. Phys Med Biol 2001;46(3):R1–45.
[28] Wright B, Summers A, Fenner J, Gillott R, Hutchinson CE, Spencer PA, et al. Initial observations using a novel "cine" magnetic resonance imaging technique to detect changes in abdominal motion caused by encapsulating peritoneal sclerosis. Perit Dial Int 2011;31(3):287–90.